

Size Effects in Thin Films of Superfluid ^3He

M. R. Freeman, R. S. Germain, E. V. Thuneberg, and R. C. Richardson

Laboratory of Atomic and Solid State Physics, Cornell University, Ithaca, New York 14853

(Received 30 October 1987)

We report the first identification of the phase of superfluid ^3He in a geometry confined on the scale of the correlation length. For a wide range of pressures and temperatures at which the B phase is stable in bulk, the A phase occurs in thin films. The order-parameter structure is deduced by nuclear magnetic resonance. Simultaneous measurements of the superfluid density monitor the magnitude of the energy gap. We demonstrate that the boundary condition on the order parameter is *tunable*. Pair breaking is reduced dramatically at surfaces covered by adsorbed monolayers of ^4He .

PACS numbers: 67.50.Fi, 67.70.+n

Anisotropic superfluids and superconductors are expected to display a variety of interesting size effects.¹ Two important consequences arise from confinement on length scales comparable to the correlation length: modification of the bulk phase diagram, and reduction of the condensate order parameter. The former is a consequence of the requirement that Cooper-pair angular momenta be oriented perpendicular to walls.² The second effect stems from the destruction of $l > 0$ (non- s -wave) Cooper pairs by *any* type of impurity scattering, as from a rough surface.³ We report studies of both effects in 300-nm-thick confined films of superfluid ^3He . Liquid ^3He is the premier system for the study of these phenomena. It remains the only realization of an unconventional superfluid or superconductor for which straightforward probes of the order parameter have been established. Simultaneous measurements of the superfluid density and NMR response of these films reveal both the nature of the ordered state and a surprising dependence of the boundary condition on the surface coverage of ^4He .

The effect of walls on the phase diagram is qualitatively similar to that of a magnetic field.⁴ A transition to a strongly anisotropic phase is expected⁵ when the film thickness, d , is reduced below about 7 times the temperature-dependent correlation length, $\xi(T)$. Well below the bulk transition temperature, T_c , ξ is essentially temperature independent but has a strong pressure dependence⁶ through which we vary the dimensionless film thickness, $d/\xi(T)$.

The predicted anisotropic phase for films depends upon the parameters used in the Ginzburg-Landau free energy.⁵ The planar and A phases are degenerate in the weak-coupling BCS case, appropriate to ^3He in the limit of zero pressure. Strong-coupling corrections stabilize the A phase at higher pressures. A qualitatively different 2D phase may exist⁷ in the region close to T_c where $\xi(T) > d$. Fortunately, the selectivity of NMR is sufficient to differentiate between these states.

The most pronounced changes in the phase diagram result directly from the confinement. Further modifications are determined by the boundary condition. Diffuse

quasiparticle scattering suppresses all components of the order parameter over a length of order ξ away from the surface. Observable quantities such as the superfluid density and transition temperature are substantially reduced in bulk values in this case.⁸ The measured parameters represent averages over the variation of the order parameter as a function of distance from the walls. Previous experimental results are qualitatively consistent with the assumption of diffuse scattering at surfaces.⁹ At specular walls, the parallel components of the order parameter survive and the bulk T_c and superfluid density should be retained.

Well-defined geometries are required before quantitative experimental information about confined superfluid ^3He can be obtained. Planar and cylindrical geometries are theoretically the most tractable, and do not confound the results of such experimental probes as NMR. The transverse NMR frequency shift depends on the relative orientation of the spin and orbital components of the order parameter.¹⁰ The walls orient the orbital degrees of freedom, and so it is desirable that all surfaces make the same angle with respect to the applied magnetic field.

Figure 1 illustrates the geometry of this experiment. A compact stack of many ^3He films is created by our filling the interstices between 3000 1.5- μm -thick Mylar sheets held 300 nm apart by polystyrene spacer beads. Mylar is a good substrate material because it is quite smooth, as characterized by studies of submonolayer superfluid ^4He films.¹¹ The spacer particles are randomly dispersed across the Mylar with an average separation of about 5 μm . This concentration of beads ensures a relatively uniform gap and at the same time is sufficiently sparse that we neglect reorientation of the order parameter near the bead surfaces.

The ^3He superfluid density is measured by the torsional-oscillator technique.¹² The manifestation of superfluidity is a decrease in the period of oscillation as the temperature is lowered and the condensate decouples from the motion of the substrate. The spacer beads play a crucial role in this regard. They are impurity scatterers which maintain equilibrium between the quasiparti-

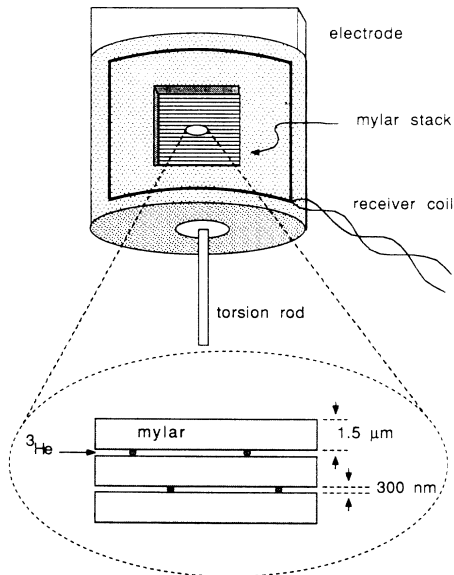


FIG. 1. Schematic picture of the cell, including a view of how the films are defined by the use of closely spaced Mylar sheets.

cle gas and the substrate, independent of the boundary condition for scattering at the Mylar surface.¹³

The torsional motion is driven and detected electrostatically. The electrodes are integrated into our crossed-coil NMR probe. An NMR detection coil is wound on the oscillator head, as shown in Fig. 1. A static magnetic field of 31 mT is applied perpendicular to the Mylar sheets. The cell is mounted on a copper nuclear demagnetization stage and can be cooled below 300 μ K. The stage temperature is measured with Pt-NMR and ^3He -melting-curve thermometers. The magnetization of the surface-adsorbed¹⁴ ^3He is used as a local thermometer for the sample.

Our measurements span pressures between 1.5 and 22 bars, with similar results in each case. We find no transition from *A* to planar or *B* phase.⁵ Representative NMR frequency shift data are shown in Fig. 2. This figure displays the information upon which the identification of *A* phase in the films is based. We plot the temperature dependence of the shift away from the Larmor resonance at 1 MHz for three different pulse amplitudes, corresponding to initial rotations of the magnetization by 30°, 90°, and 150°. A shift of (370 Hz mK)/*T* arises from a background polarization in the Mylar and has been subtracted off.

The salient characteristic of the data in Fig. 2 is the large shift in the superfluid phase, negative for tipping angles less than 90°. The observed behavior is consistent only with the *A* phase, which has a *negative* shift in the "dipole-unlocked" state¹⁵ arising in this geometry from competition between the orienting effects of walls and the magnetic field. The planar and 2D phases both have

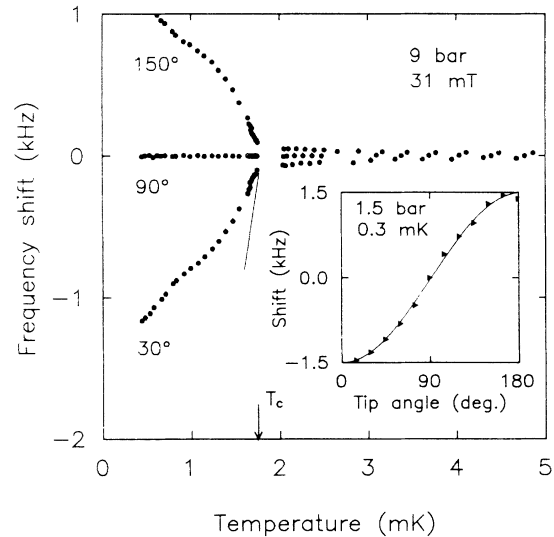


FIG. 2. Temperature dependence of the spin precession frequency of pure ^3He for several pulse angles. The unshifted Larmor resonance is at 1 MHz. The solid line represents bulk liquid response in the transition region. Inset: Tipping-angle dependence of the frequency shift.

positive frequency shifts in the continuous-wave NMR limit of small pulses.^{7,10} Our films may be too thick to display the 2D phase. We expect it only within $\approx 20 \mu\text{K}$ of the *bulk* transition. The films apparently are too thin for nucleation of the *B* phase. We expect, but do not observe, a transition at pressures above 5 bars, perhaps because of supercooling.

The large-tipping-angle, pulse-NMR response of dipole-unlocked *A* phase has not been investigated previously. The transverse resonance frequency of the superfluid is determined by¹⁰ $\omega^2 = \omega_L^2 + c\Omega^2$, where ω_L is the Larmor frequency, Ω the longitudinal resonance frequency of Leggett, and *c* a numerical factor of order unity. For the dipole-unlocked case, $c = -\cos\phi$, where ϕ is the tip angle, in contrast to the dipole-locked result,¹⁶ $c = \frac{1}{4} + \frac{3}{4}\cos\phi$. Our data agree well with the dipole-unlocked form, as shown in the inset of Fig. 2.

The *magnitude* of the frequency shift measured in our experiment is smaller than that for bulk *A* phase, as indicated by the solid line drawn in the transition region of Fig. 2. Two effects contribute to this reduction. The first is the suppression of the energy gap, which determines the frequency shift through a direct proportionality in the Ginzburg-Landau region. The second effect is an interaction with the layer of localized ^3He atoms which prevents direct measurements of the frequency of the superfluid signal. If the "solid" and liquid atoms constituted independent spin populations, we would find a double-line NMR absorption spectrum. This would be true both below T_c , where a large splitting arises from the superfluid shift, and in the normal phase at low temperatures where the dipolar shift of the solid line is

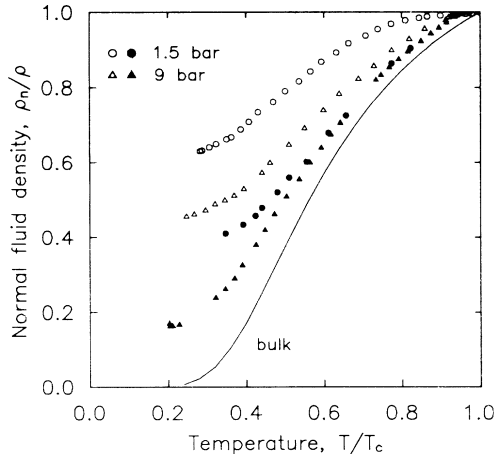


FIG. 3. Reduced normal-fluid density at 1.5 and 9 bars, each measured for two boundary conditions. The open and filled symbols correspond respectively to surfaces coated with monolayers of ^3He and ^4He . Bulk liquid data at 10 bars (Ref. 19) are plotted as the solid line.

measurable.¹⁷ We observe a solitary absorption line. The fine structure is erased by rapid spin exchange between the solid and liquid populations.¹⁸ The contributions at ω_{liq} and ω_{sol} are weighted by their relative magnetizations to determine the position, ω_{meas} , of the composite line,

$$\omega_{\text{meas}} = \omega_{\text{sol}} + \frac{M_{\text{liq}}}{M_{\text{liq}} + M_{\text{sol}}} (\omega_{\text{liq}} - \omega_{\text{sol}}).$$

The superfluid shift in Fig. 2 is therefore decreased because the dipole torque¹⁰ shifting ω_{liq} in effect acts on the total magnetization. M_{liq} is the temperature-independent Pauli magnetization of the Fermi liquid. The solid ^3He layer is a Curie-Weiss paramagnet with M_{sol} equaling M_{liq} at approximately 1.5 mK. The tipping-angle-dependent shift seen above T_c is the dipolar shift in ω_{sol} .

The effect of the boundary condition on the order parameter is graphically demonstrated in Fig. 3. The reduced normal-fluid density, ρ_n/ρ , is determined from the period shift of the oscillator in the superfluid phase, $\Delta P(T)$, normalized by the shift due to the total ^3He moment of inertia, ΔP_{fill} :

$$\frac{\rho_n}{\rho} = \frac{\Delta P(T)}{\Delta P_{\text{fill}}} \frac{1}{1 - \chi}.$$

The factor χ corrects for imperfections in the geometry,²⁰ and is obtained by calibration with superfluid ^4He . The upper two curves in Fig. 3 reflect the decrease of the correlation length with increasing pressure.⁶ In the Ginzburg-Landau model for a film with diffusely scattering surfaces,⁵ the superfluid density relative to the bulk value is

$$\rho_s/\rho_{s,\text{bulk}} = 1 - k(w)/w,$$

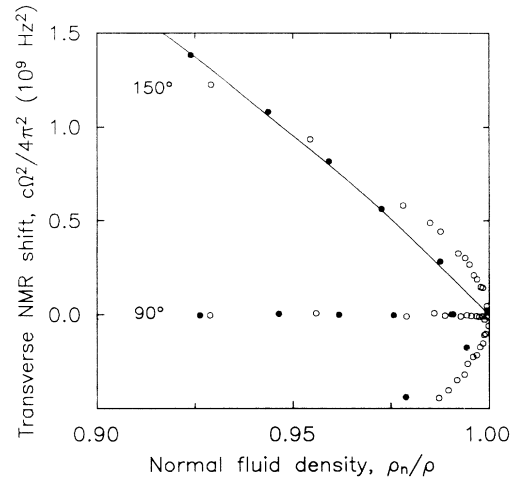


FIG. 4. Simultaneously measured quantities plotted against one another in the transition region. The solid line represents bulk behavior. This is reproduced only in the case of ^4He -covered walls (filled circles). The pure- ^3He results (open circles) suggest that the oscillator period shift is modified by flow properties and does not directly measure the superfluid density. The NMR data are corrected for the effects of the localized ^3He layer.

where $w = d/\xi(T)$ is the reduced thickness. Improving on the variational calculations,⁵ we find that $k(w)$ varies smoothly but nonmonotonically from π at the critical thickness, $w = \pi$, to 3.2 for large w . The order parameter is depressed to zero at the wall and develops its bulk amplitude over a distance of order $\xi(T)$.

The filled symbols in Fig. 3 are measured with 2 ± 1 monolayers of ^4He on the surface. The order parameter clearly has a much fuller development.²¹ Similar behavior is found for the NMR frequency shift. The most straightforward interpretation of these results is in terms of partial specularly for the boundary scattering of quasiparticles. Within the Ginzburg-Landau picture above, the effective thickness of the film increases as the scattering becomes more specular. Detailed understanding of the interaction of ^3He quasiparticles with surfaces is lacking, as indicated by recent effective-viscosity results for normal ^3He - ^4He mixtures.²²

For bulk ^3He in the Ginzburg-Landau region, both the superfluid density and the transverse NMR shift are proportional to the square of the energy gap, $\rho_s \propto \Omega^2 \propto \Delta^2$. This relationship holds approximately for the spatial averages of these quantities in the confined geometry. In Fig. 4 we plot the results of our simultaneous measurements in the transition region. The solid line represents bulk A -phase behavior at 9 bars, derived with use of a combination of available superfluid density, longitudinal resonance, and magnetic susceptibility data for the bulk B phase.¹⁹ This shape is reproduced very well for the films when the surfaces are coated with ^4He , as indicated by the filled symbols in the figure. The open symbols are

data for the cell filled with pure ^3He , in which case the superfluidity is more suppressed by the walls. The difference is plausibly explained by a breakdown of the conversion of period shift to superfluid density, due to temperature dependence of χ in the transition region. The relevance to ^3He of the χ value measured for bulk superfluid ^4He is guaranteed only when $\xi \ll d$. For diffuse surfaces, when $\xi \approx d/\pi$, superflow paths are obstructed by regions narrower than the critical thickness and inhomogeneities in the geometry therefore transform into temperature dependence of χ .

In summary, we find that the A phase is stable in thin films of superfluid ^3He . We are able to tune the boundary condition on the order parameter with adsorbed ^4He . Strengthening of the order parameter at surfaces is the key to the search for superfluidity and quantum size effects in very thin films.⁷

We have benefitted from discussions with many residents of and visitors to the Laboratory of Atomic and Solid State Physics, Cornell University, and especially thank J. M. Parpia and D. F. McQueeney. This work is supported by the National Science Foundation through Grant No. DMR 84-18605 and by the Cornell Materials Science Center, Grant No. DMR 82-17227A.

¹G. Barton and M. A. Moore, *J. Low Temp. Phys.* **21**, 489 (1975).

²V. Ambegaokar, P. G. de Gennes, and D. Rainer, *Phys. Rev. A* **9**, 2676 (1974).

³R. Balian and N. R. Werthamer, *Phys. Rev.* **131**, 1553 (1963).

⁴I. A. Privorotskii, *Phys. Rev. B* **12**, 4825 (1975).

⁵A. L. Fetter and S. Ullah, to be published; Y.-H. Li and T.-L. Ho, to be published; T. Fujita *et al.*, *Prog. Theor. Phys.* **64**, 396 (1980).

⁶K. Ichikawa *et al.*, *Phys. Rev. Lett.* **58**, 1949 (1987). At low temperatures, ξ varies from 70 nm at 0 bar to 15 nm near the melting curve.

⁷Z. Tešanović and O. T. Valls, *Phys. Rev. B* **31**, 1374 (1985), and **33**, 3139 (1986).

⁸L. H. Kjälldman, J. Kurkijärvi, and D. Rainer, *J. Low Temp. Phys.* **33**, 577 (1978).

⁹J. G. Daunt *et al.*, to be published; J. C. Davis *et al.*, *Jpn. J. Appl. Phys.* **26-3**, 147 (1987); V. Kotsubo *et al.*, *Phys. Rev. Lett.* **58**, 804 (1987).

¹⁰A. J. Leggett, *Ann. Phys. (N.Y.)* **85**, 11 (1974).

¹¹G. Agnolet, Ph.D. thesis, Cornell University, 1983 (unpublished).

¹²J. D. Reppy, in *Physics at Ultralow Temperatures*, edited by T. Sugawara (Physics Society of Japan, Tokyo, 1978).

¹³At specular surfaces without beads, no transverse momentum is exchanged and all of the helium mass is decoupled above the transition temperature. The spacer particles introduce an impurity-limited mean free path of order 50 μm , so that $\omega\tau_{\text{imp}} \approx 10^{-2}$ at 1.75 kHz, and the normal fluid is clamped.

¹⁴A. I. Ahonen *et al.*, *J. Phys. C* **9**, 1665 (1976). We see a Curie-Weiss signal equivalent to ≈ 1 layer of ^3He , unlike the ≈ 5 layers reported in this reference.

¹⁵S. Takagi, *J. Phys. C* **8**, 1507 (1975); A. I. Ahonen, M. Krusius, and M. A. Paalanen, *J. Low Temp. Phys.* **25**, 421 (1976).

¹⁶D. D. Osheroff and L. R. Corruccini, *Phys. Lett.* **51A**, 447 (1975); W. F. Brinkman and H. Smith, *Phys. Lett.* **51A**, 449 (1975).

¹⁷H. M. Bozler, D. M. Bates, and A. L. Thomson, *Phys. Rev. B* **27**, 6992 (1983).

¹⁸A. Abragam, *Principles of Nuclear Magnetism* (Oxford Univ. Press, London, 1961), Chap. 10.

¹⁹J. M. Parpia *et al.*, *J. Low Temp. Phys.* **61**, 337 (1985); P. J. Hakonen *et al.*, to be published; H. N. Scholz, Ph.D. thesis, Ohio State University, 1981 (unpublished).

²⁰M. Revzen *et al.*, *Phys. Rev. Lett.* **33**, 143 (1974).

²¹A ^4He coverage of $\frac{1}{4}$ monolayer has no effect on the ^3He superfluid density. Insight into the mechanism can be gained by further study of the coverage dependence. We vary the surface polarization but find no magnetic field dependence of the superfluid density between 0 and 30 mT.

²²D. A. Ritchie, J. Saunders, and D. F. Brewer, *Phys. Rev. Lett.* **59**, 465 (1987).

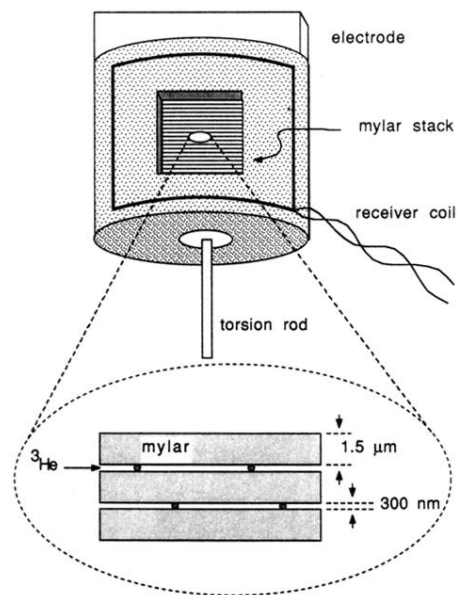


FIG. 1. Schematic picture of the cell, including a view of how the films are defined by the use of closely spaced Mylar sheets.